Published by :
http://www.ijert.org

International Journal of Engineering Research & Technology (IJERT)
ISSN: 2278-0181
Vol. 13 Issue 11, November 2024

The Study of Stability Index in High-Rise Structures with Tube-in-Tube Systems under Different Bracing Configurations and the Effects of Second-Order Analysis

Fatemeh Abdous
Ph.D Student. Department of Transportation, Morgan State University, Maryland, USA

Mohsen Gerami
Professor of Earthquake Eng. Dept., Faculty of Civil Eng., Semnan University, Semnan, Iran

***Abstract*- In high-rise structures, ensuring the lateral stability of the building is crucial to safeguarding the welfare and safety of occupants. The design must consider lateral deformations to prevent collapse and structural failure. Second-order (P-Δ) effects, induced by simultaneous axial compressive forces and bending moments on structural members, should be controlled. In designs, lateral displacements and secondary bending moments due to the P-Δ effects on members need to be taken into account. If a structure is subjected to lateral loads, the stability index of each story, which is the main criterion for structural stability, is used to assess the influence of second-order effects on the structure's height. This study examines the impact of bracing configurations and module arrangements on the stability index of high-rise tube-in-tube structures in the presence of second-order effects. Three types of bracings -X, chevron, and eccentric- are used, and all models are analyzed with and without the inclusion of P-Δ effects. The results indicate that adding bracing reduces the stability index of the tube-in-tube structure significantly, with chevron bracing having the most substantial impact. This study suggests that the coefficient for displacement modification proposed by ASCE7-05 (for braced stories) provides accurate estimations for final displacements in high-rise buildings.**

Keywords: **Tube-in-Tube System, Stability Index, High-Rise Buildings, Braced Tube, Second-Order Elastic Analysis**

1. INTRODUCTION

In designing structural members subjected to concurrent axial compression forces and bending moments, second-order (P-Δ) effects resulting from lateral deformations must be considered. These effects, induced by axial loads, produce additional bending moments and can significantly influence structural stability (Figure 1).

For structures under lateral loads, the primary bending moment in the i^{th}story denoted M_i, results from both the shear force acting on the story and the secondary moment arising due to the P-Δ effect, denoted as ΔM_i. This secondary moment ΔM_i is calculated based on the axial force P_i and the lateral displacement ΔW_i, as expressed by the relationship:

$$M_i = P_i * \Delta W_i \quad (1)$$

$$M_i = V_i * h_i \quad (2)$$

Furthermore, the stability of a story can be quantified by its stability index, θ_i,which serves as an essential criterion in high-rise structural stability analysis. Ensuring adequate lateral stiffness for buildings exposed to lateral forces becomes paramount, as excessive deformation can compromise structural integrity and occupant safety. To this end, understanding and controlling the stability index in high-rise structures, particularly when using advanced systems like tube-in-tube configurations, is essential. The ratio of the secondary moment ΔM_i (arising from the P-Δ effect) to the primary moment M_i is known as the stability coefficient of the story.

$$\theta_i = \frac{\Delta M_i}{M_i} = \left(\frac{P\Delta W}{VL}\right)_i \quad (3)$$

In this context, ΔW_i represents the initial lateral displacement at the i^{th}story, determined by the ratio of the story shear V_i to its lateral stiffness. Consequently, the final displacement is defined as:

$$\Delta_i = \frac{\Delta W_i}{1-\theta_i} \quad (4)$$

The coefficient $\frac{1}{1-\theta_i}$ serves as a conversion factor from the displacement obtained in the first-order analysis to the final displacement of the structure. This coefficient was also examined by Gupta and Krawinkler in 1999. Here, θ_i represents the stability index derived from the first-order analysis[1].

International Journal of Engineering Research & Technology (IJERT)
ISSN: 2278-0181
Vol. 13 Issue 11, November 2024

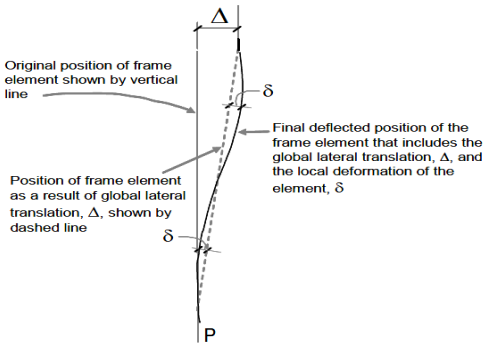

Fig -1: P.Δ and P. δ Effects

In current seismic design codes, stability indices are used to adjust the design forces for members based on each story's stability index. For tall buildings, achieving adequate stiffness, particularly lateral stiffness, is a crucial aspect of structural design. At the ultimate strength limit, lateral deformations must be controlled to prevent structural collapse from P-Δ effects[2], [3].

In this study, second-order analysis is applied to 72-story structural models with an H/B ratio of 8.16. Six tube-in-tube models with varying bracing configurations are analyzed, incorporating P-Δ effects. The results are then compared to those of a baseline 72-story tube-in-tube model, evaluating the stability index relative to the braced and unbraced tube systems.

The tube-in-tube system offers improved stability by integrating an inner core with an outer tube, which is especially effective in distributing lateral forces across both structural components. Studies have shown that tube-in-tube systems reduce the shear lag effect and manage second-order effects more effectively than conventional moment-resisting frames, leading to higher stability and reduced material usage by up to 30% [4], [5].

Further, high-rise buildings are sensitive to dynamic effects such as wind and seismic forces. Second-order effects, like P-Δ and P-δ, significantly impact the overall stability of these structures, necessitating the inclusion of innovative bracing configurations and load-distribution techniques to enhance resilience under these forces[6], [7].

This study aims to evaluate the stability coefficient of tube-in-tube high-rise buildings under different bracing systems, assessing the influence of second-order effects on structural stability. By comparing models that consider and ignore P-Δ effects, the research seeks to identify optimal configurations for minimizing lateral displacements and maximizing stability, in line with ASCE7-05 recommendations. This work ultimately contributes to refining design practices for sustainable, resilient high-rise buildings in urban environments.

2. LITERATURE REVIEW

The current body of literature on high-rise building behavior covers a broad spectrum of architectural and structural perspectives, with particular attention to sustainable design and innovative structural forms. While many studies focus on architectural and environmental considerations, research in structural dynamics, particularly regarding tube and tube-in-tube systems, provides valuable insights for understanding the complex behavior of high-rise buildings. This section highlights key advancements and findings in recent years related to high-rise structures, encompassing both architectural innovations and engineering solutions.

Although some of the reviewed literature may not be directly related to the present study, it offers relevant background for analyzing high-rise building behavior under various conditions.

Moon (2007) explored the advantages and disadvantages of high-rise building systems, detailing criteria based on current design methods, architectural considerations, and environmental conditions. One aspect examined was the impact of geometric configuration on optimizing structural weight. The study demonstrated that the angle of braces relative to the horizontal axis is a primary factor in steel weight consumption, with an increase in bracing angle up to 69 degrees reducing the steel weight, after which the weight increased[1]. In another study, Moon (2005) examined recent advancements in the implementation and control of high-rise building systems, introducing a new classification termed internal and external systems[8]. Rahgozar and colleagues (2010) studied simplified relationships for the approximate analysis of high-rise buildings with a truss cap form. By minimizing the total energy of the structure, they formulated equations to calculate lateral deformation and total axial force under three loading patterns and compared the results with SAP2000. The findings confirmed a minimal error percentage relative to analytical results[9]. Reyes and Chopra (2011) conducted an incremental load analysis on high-rise buildings by applying two simultaneous components to a three-dimensional building. As a proposed method, they introduced the Practical Multi-Point Adaptive (PMPA) incremental loading method, demonstrating that its outputs were as accurate in nonlinear analysis as spectral analysis results in linear analysis. However, linear spectral analysis caused relative displacements on lower floors of high-rise buildings to be calculated as significantly less than actual values[10].

Lu and Jiang (2011) analyzed and applied response control for high-rise structures in Mainland China. Several notable buildings in China were constructed at a reduced scale in laboratory environments and subjected to testing. Moreover, the performance of control systems, such as ATMD and controlled viscous dampers, was assessed by adjusting initial stiffness with displacement[11].

Liu and colleagues (2011) evaluated the structural performance of super-tall buildings during construction. Their findings revealed that performance levels vary at different construction stages and that the position and timing of truss cap installation can significantly improve seismic performance during construction[12]. Wang and colleagues (2011) assessed the seismic performance of columns located on transition floors in high-rise buildings through laboratory studies. The results indicated that the applied load pattern affects the ductility and failure mechanism of the specimens, with columns exhibiting acceptable behavior under monotonic loading. Additionally, SRC columns met the drift control criteria against applied seismic forces[13].

Saadatpour and Kamkar (2011) studied simplified relationships in the approximate free vibration analysis of high-rise buildings to calculate the primary vibration frequency in a tube-in-tube structure with a concrete core and truss cap. They compared the results for three different models with SAP2000, confirming minimal error percentages relative to analytical results, attributing the error to shear lag

International Journal of Engineering Research & Technology (IJERT)
ISSN: 2278-0181
Vol. 13 Issue 11, November 2024

phenomena[14]. Spence and Gioffre (2011) proposed an algorithm for optimizing reliability in high-rise buildings[15].

Maleki-Nejad and Rahgozar (2012) studied simplified relationships for calculating approximate vibration frequency and mode shapes in high-rise buildings with a tube-in-tube structure with dual truss caps. Using energy methods and Hamilton's principle, they derived the entire structure's equation and solved it by variable separation, comparing the results with SAP2000. The findings confirmed a minimal error range (1–15%) relative to analytical results[16].

Kheyroddin and colleagues (2007) studied the effect of various braced tube structural configurations on shear lag, eventually proposing an optimal relationship for determining the number of braces needed to reduce shear lag as a function of the structure's dimensions and total floors. They concluded that the fewer the braced floors (bracing modules), the more significant the reduction in shear lag. In other words, reducing the bracing angle decreases shear lag[17]. Park and Yeo (2016) analyzed second-order effects on wind-induced responses in high-rise steel structures, showing how wind loading significantly impacts drift ratios and base shears in structures with geometric stiffness designed to accommodate dynamic responses[6]. Additionally, Zu and Lam (2018) explored vortex shedding patterns using particle image velocimetry, highlighting its influence on across-wind forces and lateral stability in a high-rise building[18].

Hafner et al. (2021) studied the shear lag effect in tube structures, focusing on the uneven activation of vertical elements under horizontal loads. Their findings suggest specific design adjustments to mitigate shear lag, especially in tube structures with closely spaced exterior columns[3].

Zhang and Far (2022) investigated the impact of soil-structure interaction (SSI) on seismic performance in frame-core tube structures. Their results underscore the need to integrate SSI effects in design due to the amplified lateral displacement and inter-story drifts observed under seismic conditions[2]. Mohammadi et al. (2017) proposed a ribbed bracing system (RBSyst) to reduce buckling in braced tube systems, which enhanced stability and ductility under seismic loading[19].

Liu et al. (2024) explored the use of replaceable steel coupling beams in diagrid core-tube structures, which significantly improved energy dissipation and structural sustainability during seismic events[7].

3. GEOMETRY AND LOADING OF THE STUDIED MODELS

To examine the performance of each bracing type on the response of tall structures, 72-story buildings with various bracing forms have been analyzed. The structural system of the models includes tube-in-tube and braced tube-in-tube configurations. Initially, a 72-story model with a tube-in-tube system was developed, in which the moment frames used in both the inner and outer tubes are of the special moment-resisting frame type. Subsequently, six braced tube-in-tube models, each with different bracing forms and modules, were designed. Three types of bracing—X-bracing, chevron, and a variant of an eccentric brace (referred to as EBF in this study)—were employed. For each bracing form, two bracing modules of 8 stories and 24 stories were used. The 24-story module implies that the outer tube has a modular bracing configuration repeated every 24 stories along the building height.

The building plan has dimensions of 30 m × 30 m, with equal spans of 5 meters. The height of all floors is 3.4 meters, resulting in a height-to-width ratio (H/B) of 8:16. The building plan for the analyzed models is illustrated in Figure (2). In this plan, the outer columns form the external tube, while the inner columns form the internal tube. The diaphragms defined for the floors are rigid, ensuring connectivity and force transfer between the inner and outer tubes.

To simplify the analysis of charts and tables, each model has been assigned an identifier indicating the number of stories, bracing forms, and bracing modules in each structure. For instance, the designation T72T-X-8 represents a 72-story braced tube-in-tube structure with X-bracing and an 8-story bracing module in the outer tube. The designation T72T refers to a 72-story tube-in-tube structure without bracing (Tube 72 Tube). After creating the described models in ETABS software, they were loaded according to the provisions of Chapter 6 of the ASCE7-05 standard for lateral loads and Chapter 6 of the National Building Code for gravity loads. For gravity loading, the dead load was set to 650 kg/m², the live load to 200 kg/m², and the load for perimeter walls to 1000 kg/m. Lateral loading was based on wind loads, and the design of the structure's lateral load-resisting system was carried out under wind load conditions. Wind loading provisions followed the analytical method presented in Chapter 6 of the ASCE7-05 standard. The specifications for wind loadings used in this study are presented in Table (1)[20].

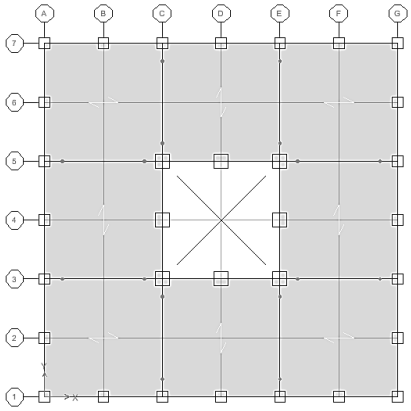

Figure-1: Models' Plan

International Journal of Engineering Research & Technology (IJERT)
ISSN: 2278-0181
Vol. 13 Issue 11, November 2024

Table-1: Wind Load Applied to the Structure in ETABS Software According to ASCE7-05 Standards

Exposure and Pressure Coefficient	Wind Exposure Parameters	Wind Coefficient
Exposure from Extents of Rigid Diaphragm	Wind Angle Relative to Axis X: 90 degrees	Basic Wind Speed: 110
	Environmental Conditions: Zone B	Wind Load Case : Case 1
	Importance Factor: 1	Force and Pressure Coefficient on Building: 1.85
	Windward Pressure Coefficient: 0.8	Topographic Factor K_z : 1
	Leeward Pressure Coefficient: 0.5	
	Load Eccentricity in Direction 1: 0	
	Load Eccentricity in Direction 2: 0	

4. CALCULATION OF STABILITY INDEX IN STRUCTURES WITH AND WITHOUT THE P-Δ EFFECT

After analyzing and designing the constructed models with consideration of the P-Δ effect and extracting the necessary parameters to calculate the stability index for each floor, the relevant parameters are presented in Tables (2) to (5). This index is calculated every 8 floors. According to the code's definition of the stability index P_i, it represents the sum of the axial force resulting from dead and live loads in all columns of floor iii and above, with ΔW_i denoting the relative displacement of each floor compared to the floor below it $(\Delta_i - \Delta_{i-1})$. Table (2) shows the stability index calculation for the X-bracing form in the 8-floor module. The stability index for other bracing configurations was calculated similarly, with the final results provided in Table (3). According to ASCE7-05, the allowable value for the stability index is limited to 0.25, which is also included in the last column of all tables in Table (2).

The stability index values for structural models without considering the P-Δ effect were also extracted in the same manner as previously described, and the results are presented in Table (4). Reviewing the values in Tables (3) and (4) shows that the stability index has a relatively uniform increase when the P-Δ effect is considered compared to when it is not. This increase is expressed in Table (5) as the ratio of the stability index with the P-Δ effect to the stability index without the P-Δ effect. As expected, this ratio is higher in unbraced tube-in-tube structures than in braced structures, with an increase of up to 1.2 times at the roof level. Generally, in braced structures, the ratio of stability index increases per floor rises with height.

The highest increase in stability index was observed in the EBF bracing with a 24-floor module, with an average increase of 1.15 times, while the lowest was observed in the chevron bracing with an 8-floor module, with a 1.116 increase. Except for the EBF bracing with a 24-floor module, which raised the stability index by 15%, other modules, and bracing forms exhibited an approximate 12% increase in stability index following applying the P-Δ effect. The stability index values for the tube-in-tube structure under second-order analysis reveal that, although the tube-in-tube structure maintains an acceptable drift angle at higher floors, the $\theta_i$index exceeds the code's permissible limit. However, employing all bracing configurations brought the index back within the allowable range. This indicates that if the drift angle of a structure is within the permissible range. Still, the stability index is outside the allowed range, using bracing can be an effective solution to address this issue.

Table-2: Stability Index in a 72-story structure with modular X-bracing, 8-floor module, considering second-order effects

Story ID	Model Name	P_i	Δw_i	v_i	h_i	θ_i	$\theta_{allowed}$
STORY 72	T72T-X-8	-1283.42	0.6464	-12.97	340	0.19	0.25
STORY 64	T72T-X-8	-11510	0.6994	-218.35	340	0.11	0.25
STORY 56	T72T-X-8	-22973.1	0.7184	-419.29	340	0.12	0.25
STORY 48	T72T-X-8	-35578	0.7137	-615.33	340	0.12	0.25
STORY 40	T72T-X-8	-48325.9	0.6793	-805.9	340	0.12	0.25
STORY 32	T72T-X-8	-61754.7	0.6133	-990.19	340	0.11	0.25
STORY 24	T72T-X-8	-75384	0.5281	-1167.11	340	0.10	0.25

International Journal of Engineering Research & Technology (IJERT)
ISSN: 2278-0181
Vol. 13 Issue 11, November 2024

STORY 16	T72T-X-8	-89855.2	0.4175	-1334.9	340	0.08	0.25
STORY 8	T72T-X-8	-105058	0.2977	-1490.16	340	0.06	0.25
STORY 1	T72T-X-8	-118089	0.0517	-1607.9	340	0.01	0.25

TABLE UNIT: TON-CM

Table-3: Stability Index in 72-story structures with second-order effects

Story ID	T72T-X-8	T72T-X-24	T72T-INV-8	T72T-INV-24	T72T-EBF-8	T72T-EBF-24	T72T
STORY 72	0.19	0.12	0.19	0.06	0.10	0.14	0.28
STORY 64	0.11	0.06	0.11	0.07	0.10	0.09	0.18
STORY 56	0.12	0.07	0.12	0.12	0.12	0.11	0.18
STORY 48	0.12	0.10	0.12	0.10	0.13	0.10	0.17
STORY 40	0.12	0.09	0.12	0.10	0.13	0.11	0.16
STORY 32	0.11	0.08	0.11	0.12	0.13	0.12	0.14
STORY 24	0.10	0.11	0.10	0.10	0.12	0.10	0.12
STORY 16	0.08	0.08	0.08	0.05	0.10	0.09	0.11
STORY 8	0.06	0.06	0.06	0.07	0.08	0.07	0.08
STORY 1	0.01	0.01	0.01	0.01	0.02	0.02	0.02

5. EXAMINATION OF STABILITY INDEX VARIATIONS IN TALL BUILDINGS ALONG BUILDING HEIGHT

To investigate the variations in the stability index along the building height, we first review the results in Table (4). A closer examination of the values in Table (4) reveals that qualitative changes in the stability index along the height of the structure are more dependent on the bracing module than the bracing form. In other words, the increase or decrease in the stability index for the 8-floor module is more similar across different bracing types, such as X-bracing, Chevron, and EBF, than the stability index changes in the X-bracing form between the 8-floor and 24-floor modules.

Table-4: Stability Index in 72-story structures without second-order effects

Story ID	T72T-X-8	T72T-X-24	T72T-INV-8	T72T-INV-24	T72T-EBF-8	T72T-EBF-24	T72T
STORY 72	0.16	0.11	0.17	0.05	0.08	0.12	0.23
STORY 64	0.09	0.05	0.10	0.06	0.10	0.08	0.15
STORY 56	0.10	0.06	0.10	0.10	0.10	0.09	0.15
STORY 48	0.11	0.09	0.10	0.09	0.11	0.09	0.14
STORY 40	0.10	0.08	0.10	0.08	0.11	0.10	0.13

International Journal of Engineering Research & Technology (IJERT)
ISSN: 2278-0181
Vol. 13 Issue 11, November 2024

STORY 32	0.10	0.07	0.10	0.10	0.11	0.10	0.12
STORY 24	0.09	0.09	0.09	0.09	0.10	0.09	0.11
STORY 16	0.07	0.07	0.07	0.06	0.09	0.08	0.09
STORY 8	0.06	0.05	0.06	0.05	0.07	0.06	0.07
STORY 1	0.01	0.01	0.01	0.01	0.02	0.02	0.02

Table-5: Ratio of Stability Index with Second-Order Analysis to Stability Index with First-Order Analysis

Story ID	**T72T-X-8**	**T72T-X-24**	**T72T-INV-8**	**T72T-INV-24**	**T72T-EBF-8**	**T72T-EBF-24**	**T72T**
STORY 72	1.15	1.15	1.14	1.14	1.16	1.17	1.2
STORY 64	1.15	1.15	1.14	1.15	1.00	1.16	1.2
STORY 56	1.15	1.14	1.14	1.17	1.16	1.17	1.2
STORY 48	1.15	1.15	1.14	1.16	1.16	1.17	1.19
STORY 40	1.15	1.14	1.14	1.15	1.16	1.17	1.18
STORY 32	1.14	1.14	1.14	1.16	1.16	1.17	1.17
STORY 24	1.13	1.15	1.13	1.16	1.15	1.16	1.16
STORY 16	1.12	1.13	1.12	1.12	1.14	1.15	1.14
STORY 8	1.1	1.09	1.09	1.07	1.11	1.11	1.11
STORY 1	1.00	0.99	0.99	0.98	1.03	1.04	1.05
AVERAG E	1.122	1.123	1.116	1.126	1.122	1.146	1.162

The values in Table (4) are plotted as two charts in Figure (3) for the 8-floor module with different bracing forms, and in Figure (4) for the 24-floor module with different bracing forms. Given the relatively uniform difference in stability index between the cases with and without the P-Δ effect, the qualitative results of stability index changes along the height are similar for both analyses. Therefore, this section focuses only on the charts for the analysis with the P-Δ effect.

We begin with the 8-floor bracing module. As shown in Figure (3), the stability index values in the X-bracing and Chevron forms are very close and, in some cases, overlap. Since the stability index is directly related to relative lateral displacement and axial force in the columns, the axial force in the columns is also examined. The analysis shows that the axial force in the columns for the X-bracing form is lower than in the Chevron bracing form. This is because X-bracing, due to its higher stiffness compared to Chevron bracing, absorbs more lateral forces, reducing the forces in the columns. The relative displacement of floors in the X-bracing form is also found to be greater than in the Chevron form, which can be attributed to the section size of the Chevron bracing in the 72-story structure. The lower stiffness of Chevron bracing compared to X-bracing necessitates the use of heavier sections in the Chevron form, resulting in smaller average displacements in Chevron bracing compared to X-bracing in the studied models.

In summary, in X-bracing, the axial forces in the columns are lower than in Chevron bracing, and the relative floor displacements are higher than in Chevron bracing. The product of these two parameters for calculating the stability index brings the stability index values closer for these two bracing forms.

International Journal of Engineering Research & Technology (IJERT)
ISSN: 2278-0181
Vol. 13 Issue 11, November 2024

The general behavior of the EBF bracing is similar to the X-bracing and Chevron forms, with only a slight increase in the stability index for EBF bracing compared to X-bracing and Chevron.

In all three bracing forms, the stability index increases up to the 48th floor (67% of the building height), then slightly decreases or stabilizes up to 90% of the building height. Beyond 90% of the height, the stability index increases again. The increase in stability index from the base to 67% of the height can be attributed to the increase in relative lateral displacement up to this level. The drift angle curves for moment-resisting frames indicate that the drift angle predominantly increases in the lower 50% of the building height. According to Equation (1), the stability index can be seen as a coefficient of the drift angle in each floor, multiplied by the P/V constant for the same floor. Therefore, the stability index curves should closely resemble the drift angle curves for each floor, as shown in Figures (3) and (4).

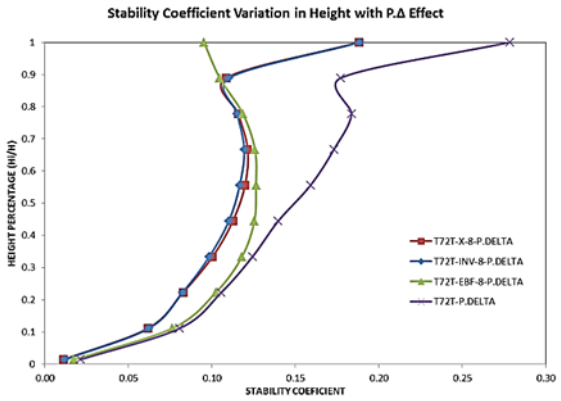

Figure-3: Variations in the Stability Index along Building Height Considering the P-Δ Effect in the Structure with an 8-Story Module

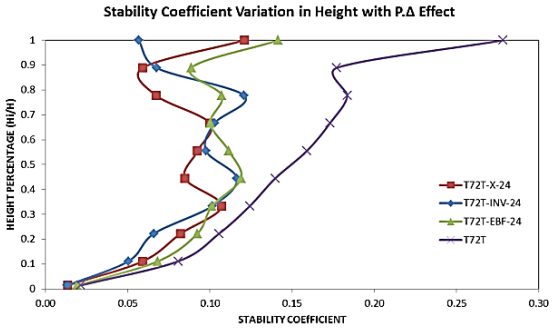

Figure-4: Variations in the Stability Index along Building Height Considering the P-Δ Effect in the Structure with a 24-Story Module

In the range from 67% to 90% of the height, the relative displacement does not vary significantly, resulting in a stable or slightly decreasing stability index in this range. In the final 10% of the building height, the main factor for the increase in stability index in X-bracing and Chevron bracing is the sharp reduction in floor shear. For EBF bracing, in addition to the reduction in floor shear, there is also a considerable decrease in the axial force of columns due to the high stiffness of the bracing, leading to minimal changes in the stability index.

Given the importance of lateral stiffness in calculating the stability index, it is evident that the designed sections have a significant impact on this index. To examine the stability index in the 24-floor module, we analyze Figure (4). The data for the 24-floor module in X-bracing from Tables (3) and (4) indicate that the stability index follows a periodic ascending trend, aligned with the bracing module. This means that in the 24-floor module, the stability index initially increases from the first to the 24th floor, then decreases, and increases again in the next 24 floors, from the 24th to the 48th floor. This trend suggests the presence of discontinuities in stiffness, as the structure experiences a reduction in stiffness at the start and end of each bracing module. For instance, in the 72-story structure with a 24-floor modular bracing, these stiffness reductions occur on the 24th and 48th floors.

In the Chevron and EBF bracing forms, a similar, but less regular, pattern is observed. In Chevron bracing, the increase in stability index is visible up to the 32nd floor. It should be noted that in the unbraced tube-in-tube structure, the stability index increases with building height. Table (6) shows the stability index ratio for each bracing configuration compared to the baseline model.

Additionally, Table (7) presents the percentage reduction in stability index for each bracing configuration compared to the baseline model. It is observed that X-bracing achieved the greatest reduction in stability index, with an average reduction of 40.97%, while the EBF bracing with an 8-floor module showed the smallest impact, with a reduction of 23.31%.

Table-6: Stability Index Ratio in Braced Structures Compared to Tube-in-Tube System with Second-Order Effects

Story ID	T72T-X-8	T72T-X-24	T72T-INV-8	T72T-INV-24	T72T-EBF-8	T72T-EBF-24
STORY 72	0.68	0.43	0.68	0.20	0.34	0.51
STORY 64	0.61	0.33	0.62	0.38	0.59	0.50
STORY 56	0.63	0.37	0.63	0.66	0.65	0.58
STORY 48	0.70	0.58	0.69	0.59	0.73	0.58

International Journal of Engineering Research & Technology (IJERT)
ISSN: 2278-0181
Vol. 13 Issue 11, November 2024

STORY 40	0.75	0.58	0.73	0.61	0.79	0.70
STORY 32	0.81	0.61	0.79	0.83	0.90	0.85
STORY 24	0.81	0.86	0.79	0.82	0.95	0.81
STORY 16	0.78	0.78	0.78	0.62	0.97	0.88
STORY 8	0.76	0.73	0.77	0.62	0.95	0.85
STORY 1	0.52	0.63	0.56	0.63	0.81	0.90

Table-7: Percentage Reduction (%) in Stability Index in Braced Structures Compared to Tube-in-Tube System with Second-Order Effects

Story ID	**T72T-X-8**	**T72T-X-24**	**T72T-INV-8**	**T72T-INV-24**	**T72T-EBF-8**	**T72T-EBF-24**
STORY 72	32.40	56.56	32.22	79.64	65.77	49.12
STORY 64	38.78	66.67	37.85	61.81	40.92	49.99
STORY 56	36.94	63.34	37.29	34.18	35.43	41.53
STORY 48	29.85	42.23	31.02	40.54	27.3	42.07
STORY 40	24.68	41.86	26.68	38.67	20.52	29.89
STORY 32	19.48	39.32	21.17	16.65	10.24	14.88
STORY 24	19.27	13.81	20.83	18.28	5.07	18.50
STORY 16	21.69	22.13	21.96	37.51	3.05	12.50
STORY 8	23.55	26.77	22.97	37.63	5.42	15.28
STORY 1	47.63	36.97	43.94	37.3	19.39	10.26
AVERAGE	29.43	40.97	29.59	40.22	23.31	28.40

Figure (5) plots the stability index variations for cases with and without the P-Δ effect. As shown in Figure (5), second-order effects do not significantly alter the stability index in the first 10% of the building height from the base level. This observation is independent of the bracing form.

6. CALCULATION OF LATERAL DISPLACEMENTS IN FIRST-ORDER AND SECOND-ORDER ANALYSIS

In this section, using the stability index for each floor in the first-order analysis of the studied models, the coefficient $\frac{1}{1-\theta_i}$ is first calculated. Then, the final lateral displacement of the structure is calculated according to Equation (1). This displacement is then compared with the final displacement of the structure, considering the P-Δ effect in the analysis. The results for different bracing configurations are presented in Tables (8) to (14).

Published by :
http://www.ijert.org

International Journal of Engineering Research & Technology (IJERT)
ISSN: 2278-0181
Vol. 13 Issue 11, November 2024

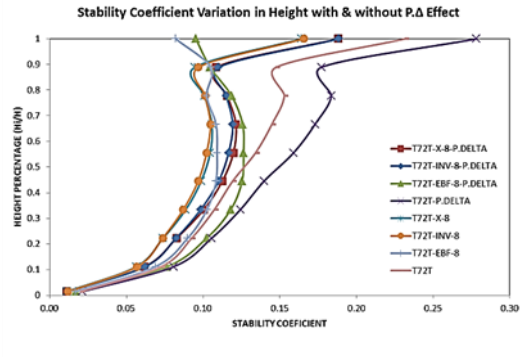

Figure-5: Stability Index Variations Along Building Height With and Without P-Δ Effect for the 8-Floor Module

Table-8: Comparison of Lateral Displacement in Tube-in-Tube Structure in Second-Order Analysis and Applying the Coefficient $\frac{1}{1-\theta_i}$

Story ID	Model Name	Δw_i	θ_i	$\frac{1}{1-\theta_i}$	Δ_i	$\Delta_i - P.\Delta$	Variation %
STORY 72	T72T	0.5798	0.23	1.3	0.75	0.70	-8.41
STORY 64	T72T	0.6911	0.15	1.17	0.81	0.83	2.22
STORY 56	T72T	0.7212	0.15	1.18	0.85	0.87	1.68
STORY 48	T72T	0.6858	0.14	1.17	0.80	0.82	2.09
STORY 40	T72T	0.63	0.13	1.16	0.73	0.75	2.52
STORY 32	T72T	0.5506	0.12	1.14	0.63	0.65	3.09
STORY 24	T72T	0.4839	0.11	1.12	0.54	0.56	3.29
STORY 16	T72T	0.405	0.09	1.10	0.45	0.46	3.42
STORY 8	T72T	0.3065	0.07	1.08	0.33	0.34	3.11
STORY 1	T72T	0.0822	0.02	1.02	0.08	0.09	3.12

Table-9: Comparison of Lateral Displacement in Tubular Structure with 8-story Modular X-Bracing in Second-Order Analysis and Applying the Coefficient $\frac{1}{1-\theta_i}$

Story ID	Model Name	Δw_i	θ_i	$\frac{1}{1-\theta_i}$	Δ_i	$\Delta_i - P.\Delta$	Variation %
STORY 72	T72T-X-8	0.5643	0.16	1.20	0.68	0.65	-4.45
STORY 64	T72T-X-8	0.6101	0.09	1.10	0.67	0.70	3.65
STORY 56	T72T-X-8	0.6261	0.10	1.11	0.70	0.72	3.07
STORY 48	T72T-X-8	0.6220	0.11	1.12	0.70	0.71	2.54
STORY 40	T72T-X-8	0.5931	0.10	1.12	0.66	0.68	2.49
STORY 32	T72T-X-8	0.5380	0.10	1.11	0.60	0.61	2.67
STORY 24	T72T-X-8	0.4665	0.09	1.10	0.51	0.53	3.07

International Journal of Engineering Research & Technology (IJERT)
ISSN: 2278-0181
Vol. 13 Issue 11, November 2024

STORY 16	T72T-X-8	0.3734	0.07	1.08	0.40	0.42	3.42
STORY 8	T72T-X-8	0.2718	0.06	1.06	0.29	0.30	3.25
STORY 1	T72T-X-8	0.0518	0.01	1.01	0.05	0.05	-1.33

STORY 16	T72T-X-24	0.4180	0.07	1.08	0.4509	0.4704	4.14
STORY 8	T72T-X-24	0.2927	0.05	1.06	0.3095	0.3197	3.20
STORY 1	T72T-X-24	0.0694	0.01	1.01	0.0704	0.0686	-2.56

Table-10: Comparison of Lateral Displacement in Tubular Structure with 24-story Modular X-Bracing in Second-Order Analysis and Applying the Coefficient $\frac{1}{1-\theta_i}$

Story ID	**Model Name**	Δw_i	θ_i	$\frac{1}{1-\theta_i}$	Δ_i	$\Delta_i - P.\Delta$	**Variation %**
STORY 72	T72T-X-24	0.3871	0.11	1.12	0.4326	0.4451	2.81
STORY 64	T72T-X-24	0.5588	0.05	1.05	0.5891	0.6406	8.03
STORY 56	T72T-X-24	0.5389	0.06	1.06	0.5726	0.6161	7.06
STORY 48	T72T-X-24	0.6402	0.09	1.09	0.7009	0.7393	5.20
STORY 40	T72T-X-24	0.5603	0.08	1.09	0.6096	0.6404	4.81
STORY 32	T72T-X-24	0.4894	0.07	1.08	0.5288	0.5565	4.97
STORY 24	T72T-X-24	0.5628	0.09	1.10	0.6206	0.6469	4.06

Table-11: Comparison of Lateral Displacement in Tubular Structure with 8-story Modular Chevron Bracing in Second-Order Analysis and Applying the Coefficient $\frac{1}{1-\theta_i}$

Story ID	**Model Name**	Δw_i	θ_i	$\frac{1}{1-\theta_i}$	Δ_i	$\Delta_i - P.\Delta$	**Variation %**
STORY 72	T72T-INV-∞	0.4726	0.17	1.20	0.5664	0.5384	-5.20
STORY 64	T72T-INV-∞	0.5321	0.10	1.11	0.5893	0.6040	2.44
STORY 56	T72T-INV-∞	0.5600	0.10	1.11	0.6231	0.6364	2.09
STORY 48	T72T-INV-∞	0.5682	0.10	1.12	0.6347	0.6473	1.95
STORY 40	T72T-INV-∞	0.5510	0.10	1.11	0.6138	0.6280	2.26
STORY 32	T72T-INV-∞	0.5078	0.10	1.11	0.5622	0.5776	2.66
STORY 24	T72T-INV-∞	0.4446	0.09	1.10	0.4870	0.5027	3.13

International Journal of Engineering Research & Technology (IJERT)
ISSN: 2278-0181
Vol. 13 Issue 11, November 2024

STORY 16	T72T-INV-∞	0.3656	0.07	1.08	0.3947	0.4089	3.48
STORY 8	T72T-INV-∞	0.2738	0.06	1.06	0.2903	0.2992	2.97
STORY 1	T72T-INV-∞	0.059	0.01	1.01	0.0597	0.0582	-2.62

STORY 16	T72T-INV-24	0.3614	0.06	1.06	0.38	0.41	5.43
STORY 8	T72T-INV-24	0.2879	0.05	1.05	0.30	0.31	2.34
STORY 1	T72T-INV-24	0.0782	0.01	1.01	0.08	0.08	-3.23

Table-12: Comparison of Lateral Displacement in Tubular Structure with 24-story Modular Chevron Bracing in Second-Order Analysis and Applying the Coefficient $\frac{1}{1-\theta_i}$

Story ID	**Model Name**	Δw_i	θ_i	$\frac{1}{1-\theta_i}$	Δ_i	$\Delta_i - P.\Delta$	**Variation %**
STORY 72	T72T-INV-24	0.1334	0.05	1.05	0.14	0.15	7.58
STORY 64	T72T-INV-24	0.4624	0.06	1.06	0.49	0.53	7.32
STORY 56	T72T-INV-24	0.6304	0.10	1.12	0.70	0.74	4.33
STORY 48	T72T-INV-24	0.5373	0.09	1.10	0.59	0.62	5.14
STORY 40	T72T-INV-24	0.5404	0.08	1.09	0.59	0.62	5.39
STORY 32	T72T-INV-24	0.5735	0.10	1.11	0.64	0.67	4.29
STORY 24	T72T-INV-24	0.4878	0.09	1.10	0.53	0.57	5.37

Table-13: Comparison of Lateral Displacement in Tubular Structure with 8-Story Modular EBF Bracing in Second-Order Analysis and Applying the Coefficient $\frac{1}{1-\theta_i}$

Story ID	**Model Name**	Δw_i	θ_i	$\frac{1}{1-\theta_i}$	Δ_i	$\Delta_i - P.\Delta$	**Variation %**
STORY 72	T72T-EBF-8	0.4519	0.08	1.09	0.4923	0.5241	6 .06
STORY 64	T72T-EBF-8	0.6102	0.10	1.12	0.6817	0.6087	11.99
STORY 56	T72T-EBF-8	0.5781	0.10	1.11	0.6440	0.6695	3.81
STORY 48	T72T-EBF-8	0.5917	0.11	1.12	0.6637	0.6864	3.31
STORY 40	T72T-EBF-8	0.5685	0.11	1.12	0.6381	0.6585	3.09
STORY 32	T72T-EBF-8	0.5574	0.11	1.12	0.6252	0.6447	3.03
STORY 24	T72T-EBF-8	0.5098	0.10	1.11	0.5680	0.5866	3.16

International Journal of Engineering Research & Technology (IJERT)
ISSN: 2278-0181
Vol. 13 Issue 11, November 2024

STORY 16	T72T-EBF-8	0.4343	0.09	1.10	0.4772	0.4941	3.42
STORY 8	T72T-EBF-8	0.3201	0.07	1.07	0.3438	0.3550	3.16
STORY 1	T72T-EBF-8	0.0757	0.02	1.02	0.0770	0.0778	1.04

Table-14: Comparison of Lateral Displacement in Tubular Structure with 24-story Modular EBF Bracing in Second-Order Analysis and Applying the Coefficient $\frac{1}{1-\theta_i}$

Story ID	**Model Name**	Δw_i	θ_i	$\frac{1}{1-\theta_i}$	Δ_i	$\Delta_i - P.\Delta$	**Variation %**
STORY 72	T72T-EBF-24	0.3675	0.12	1.14	0.4179	0.4315	3.15
STORY 64	T72T-EBF-24	0.5207	0.08	1.08	0.5637	0.6045	6.75
STORY 56	T72T-EBF-24	0.5612	0.09	1.10	0.6181	0.6548	5.61
STORY 48	T72T-EBF-24	0.5532	0.09	1.09	0.6052	0.6451	6.18
STORY 40	T72T-EBF-24	0.5665	0.10	1.11	0.6263	0.6617	5.35
STORY 32	T72T-EBF-24	0.5553	0.10	1.11	0.6183	0.6482	4.61
STORY 24	T72T-EBF-24	0.5142	0.09	1.10	0.5633	0.5975	5.72
STORY 16	T72T-EBF-24	0.446	0.08	1.09	0.4851	0.5116	5.19
STORY 8	T72T-EBF-24	0.3504	0.06	1.07	0.3734	0.3889	3.98
STORY 1	T72T-EBF-24	0.0986	0.02	1.02	0.1005	0.1023	1.81

Table-15: Comparison of Displacement Variations in Second-Order Analysis and Applying the Coefficient $\frac{1}{1-\theta_i}$

Story ID	**T72T-X-8**	**T72T-X-24**	**T72T-INV-8**	**T72T-INV-24**	**T72T-EBF-8**	**T72T-EBF-24**	**T72T**
STORY 72	-4.45	2.81	-5.20	7.58	6 .06	3.15	-8.41
STORY 64	3.65	8.03	2.44	7.32	11.99	6.75	2.22
STORY 56	3.07	7.06	2.09	4.33	3.81	5.61	1.68
STORY 48	2.54	5.20	1.95	5.14	3.31	6.18	2.09
STORY 40	2.49	4.81	2.26	5.39	3.09	5.35	2.52

International Journal of Engineering Research & Technology (IJERT)
ISSN: 2278-0181
Vol. 13 Issue 11, November 2024

STORY 32	2.67	4.97	2.66	4.29	3.03	4.61	3.09
STORY 24	3.07	4.06	3.13	5.37	3.16	5.72	3.29
STORY 16	3.42	4.14	3.48	5.43	3.42	5.19	3.42
STORY 8	3.25	3.20	2.97	2.34	3.16	3.98	3.11
STORY 1	-1.33	-2.56	-2.62	-3.23	1.04	1.81	3.12
AVERAGE(%)	1.84	4.17	1.32	4.4	1.81	4.84	1.61

Figure (6) shows the acceptable alignment of relative lateral displacement of floors under the effect of P-Δ analysis and using the displacement conversion coefficient in the 24-story modular X-bracing configuration.

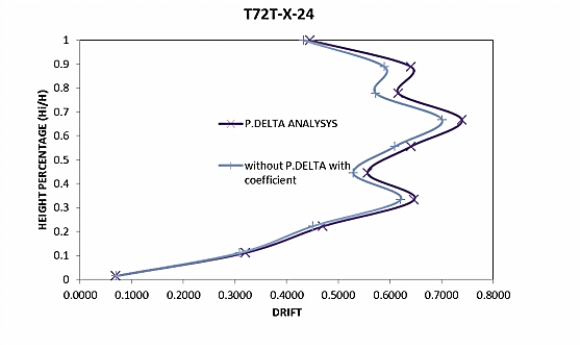

Figure-6: Comparison of Relative Displacement of Floors Between the Case Considering P-Δ Effects in Analysis and Applying the Coefficient $\frac{1}{1-\theta_i}$ in First-Order Effects

7. CONCLUSION

The use of a modular braced tube-in-tube structural form to address the weaknesses of the tube-in-tube system has only been explored in a limited number of studies. To increase lateral stiffness and reduce both inter-story and overall drift angles, various modular bracing configurations (where the bracing is repeated over several floors) have been proposed, with most previous studies focusing on diagonal or X-bracing forms. One critical aspect of tall buildings is their stability, which is often defined by the floor stability index. This study aims to evaluate the effects of different mega-bracing configurations (X-bracing, Chevron, and EBF) on the seismic demands of tall buildings, as well as the impacts of secondary moments on the stability index and the relative displacement requirements. Additionally, the possibility of using first-order elastic analysis results with a displacement amplification factor, based on the floor stability index, is examined.

The main findings regarding the stability index in 72-story structures are as follows:

1. Including P-Δ effects in the calculations leads to an increase in the stability index. This increase is relatively uniform across all bracing configurations and is approximately 12%.
2. Changes in the stability index along the building height are more dependent on the bracing module than on the bracing form. For example, structures with X-bracing, Chevron, and EBF bracing in the 8-floor module exhibit similar behavior, while the same bracing forms in the 24-floor module also show similar behavior to each other.
3. In unbraced tube-in-tube structures, the stability index increases along the building height.
4. In tube-in-tube structures considering P-Δ effects, the stability index in the upper floors exceeds the permissible range in the code, despite maintaining an acceptable drift angle. However, using any bracing configuration restores the stability index to within the permissible range. This suggests that if the drift angle of a structure is within the acceptable range, but the stability index is not, using bracing is an effective solution to address this issue by increasing lateral stiffness.
5. The variations in the stability index along the building height resemble the variations in the drift angle of floors along the building height.
6. In the 8-floor module, the stability index increases up to 67% of the building height (H0-67%), which is influenced by the increase in drift at this height. Between 67% and 90% of the height (H67%-H90%), the stability index remains almost constant or slightly decreases. Above 90% of the height, the stability index rises again due to a reduction in floor shear within this range.
7. In the initial 10% of the building height (H10%), the stability index changes are almost independent of the bracing form and even of the inclusion of P-Δ effects in the calculations.
8. In the 24-floor X-bracing module, the stability index follows a periodic ascending trend corresponding to the bracing module. This means that the stability index initially increases from the first to the 24th floor, then decreases, and rises again from the 24th to the 48th floor. This pattern indicates stiffness discontinuities, as the structure experiences a reduction in stiffness at the start and end of each bracing module. Similar, though irregular, behavior is observed in Chevron and EBF bracing configurations.
9. The final displacements of the structure were calculated using the two methods discussed in Section 5. The results from these two methods showed very good alignment, with greater consistency for the 8-floor module than for the 24-floor module.

International Journal of Engineering Research & Technology (IJERT)
ISSN: 2278-0181
Vol. 13 Issue 11, November 2024

8. REFERENCES

[1] M. M. Ali and K. S. Moon, "Structural Developments in Tall Buildings: Current Trends and Future Prospects," Architectural Science Review, vol. 50, no. 3, pp. 205–223, Sep. 2007, doi: 10.3763/asre.2007.5027.

[2] X. Zhang and H. Far, "Seismic behaviour of high-rise frame-core tube structures considering dynamic soil–structure interaction," Bull Earthquake Eng, vol. 20, no. 10, pp. 5073–5105, Aug. 2022, doi: 10.1007/s10518-022-01398-9.

[3] I. Hafner, A. Vlašić, T. Kišiček, and T. Renić, "Parametric Analysis of the Shear Lag Effect in Tube Structural Systems of Tall Buildings," Applied Sciences, vol. 11, no. 1, p. 278, Dec. 2020, doi: 10.3390/app11010278.

[4] Bipin H Naik, B S Suresh Chandra, "Comparative Analysis between Tube in Tube Structure and Conventional Moment Resisting Frame," IRJET, vol. 04, no. 10, Oct. 2017.

[5] Lavanya.T, Sathyanarayana Sridhar.R, "DYNAMIC ANALYSIS OF TUBE-IN-TUBE TALL BUILDINGS," vol. 04, no. 04, Apr. 2017, [Online]. Available: https://www.irjet.net/archives/V4/i4/IRJET-V4I4593.pdf

[6] S. Park and D. Yeo, "Database-assisted Design and second-order effects on the wind-induced structural behavior of high-rise steel buildings," National Institute of Standards and Technology, NIST TN 1940, Oct. 2016. doi: 10.6028/NIST.TN.1940.

[7] C. Liu, G. Li, B. He, C. Zhou, and Y. Ma, "Sustainable Seismic Performance of Diagrid Core-Tube Structure with Replaceable Steel Coupling Beam," Sustainability, vol. 16, no. 7, p. 2690, Mar. 2024, doi: 10.3390/su16072690.

[8] K.-S. Moon, "Dynamic Interrelationship between Technology and Architecture in Tall Buildings," Jan. 2005.

[9] R. Rahgozar, A. R. Ahmadi, and Y. Sharifi, "A simple mathematical model for approximate analysis of tall buildings," Applied Mathematical Modelling, vol. 34, no. 9, pp. 2437–2451, Sep. 2010, doi: 10.1016/j.apm.2009.11.009.

[10] J. C. Reyes and A. K. Chopra, "Three-dimensional modal pushover analysis of buildings subjected to two components of ground motion, including its evaluation for tall buildings," Earthq Engng Struct Dyn, vol. 40, no. 7, pp. 789–806, Jun. 2011, doi: 10.1002/eqe.1060.

[11] X. L. Lu and H. J. Jiang, "Research and Practice of Response Control for Tall Buildings in Mainland China," Procedia Engineering, vol. 14, pp. 73–83, 2011, doi: 10.1016/j.proeng.2011.07.008.

[12] N. X. Liu, X. Zhao, H. H. Sun, Y. M. Zheng, and J. M. Ding, "Structural Performance Assessment and Control of Super Tall Buildings During Construction," Procedia Engineering, vol. 14, pp. 2503–2510, 2011, doi: 10.1016/j.proeng.2011.07.315.

[13] W. Wang, Y. Chen, B. Dong, and R. T. Leon, "Experimental behavior of transfer story connections for high-rise SRC structures under seismic loading," Earthq Engng Struct Dyn, vol. 40, no. 9, pp. 961–975, Jul. 2011, doi: 10.1002/eqe.1067.

[14] R. Kamgar and M. M. Saadatpour, "A simple mathematical model for free vibration analysis of combined system consisting of framed tube, shear core, belt truss and outrigger system with geometrical discontinuities," Applied Mathematical Modelling, vol. 36, no. 10, pp. 4918–4930, Oct. 2012, doi: 10.1016/j.apm.2011.12.029.

[15] S. M. J. Spence and M. Gioffrè, "Efficient algorithms for the reliability optimization of tall buildings," Journal of Wind Engineering and Industrial Aerodynamics, vol. 99, no. 6–7, pp. 691–699, Jun. 2011, doi: 10.1016/j.jweia.2011.01.017.

[16] M. Malekinejad and R. Rahgozar, "A simple analytic method for computing the natural frequencies and mode shapes of tall buildings," Applied Mathematical Modelling, vol. 36, no. 8, pp. 3419–3432, Aug. 2012, doi: 10.1016/j.apm.2011.10.018.

[17] R. Zahiri-Hashemi, A. Kheyroddin, and B. Farhadi, "Effective number of mega-bracing, in order to minimize shear lag," Structural Engineering and Mechanics, vol. 48, no. 2, pp. 173–193, Oct. 2013, doi: 10.12989/SEM.2013.48.2.173.

[18] G. Zu and K. M. Lam, "Simultaneous measurement of wind velocity field and wind forces on a square tall building," Advances in Structural Engineering, vol. 21, no. 15, pp. 2241–2258, Nov. 2018, doi: 10.1177/1369433218770822.

[19] H. Mohammadi, V. Toufigh, A. A. Golafshani, and A. Arzeytoon, "Performance-based assessment of an innovative braced tube system for tall buildings," Bull Earthquake Eng, vol. 16, no. 2, pp. 731–752, Feb. 2018, doi: 10.1007/s10518-017-0219-2.

[20] Structural Engineering Institute, Ed., Minimum design loads for buildings and other structures, 6. print., Includes Suppl. No. 1 and Errata. in ASCE standard, no. ASCE/SEI 7-05. Reston, Va.: American Society of Civil Engineers, 2006.